

Altered distribution of mitochondria impairs calcium homeostasis in rat hippocampal neurons in culture

Guang Jian Wang,¹ Joshua G. Jackson and Stanley A. Thayer

Department of Pharmacology, University of Minnesota Medical School, Minneapolis, Minnesota, USA

Abstract

The specificity of Ca²⁺ signals is conferred in part by limiting changes in cytosolic Ca²⁺ to subcellular domains. Mitochondria play a major role in regulating Ca²⁺ in neurons and may participate in its spatial localization. We examined the effects of changes in the distribution of mitochondria on NMDA-induced Ca²⁺ increases. Hippocampal cultures were treated with the microtubule-destabilizing agent vinblastine, which caused the mitochondria to aggregate and migrate towards one side of the neuron. This treatment did not appear to decrease the energy status of mitochondria, as indicated by a normal membrane potential and pH gradient across the inner membrane. Moreover, electron microscopy showed that vinblastine treatment altered the distribution but not the ultrastructure of mitochondria. NMDA (200 μM, 1 min) evoked a

greater increase in cytosolic Ca²⁺ in vinblastine-treated cells than in untreated cells. This increase did not result from impaired Ca²⁺ efflux, enhanced Ca²⁺ influx, opening of the mitochondrial permeability transition pore or altered function of endoplasmic reticulum Ca²⁺ stores. Ca²⁺ uptake into mitochondria was reduced by 53% in vinblastine-treated cells, as reported by mitochondrially targeted aequorin. Thus, the distribution of mitochondria maintained by microtubules is critical for buffering Ca²⁺ influx. A subset of mitochondria close to a Ca²⁺ source may preferentially regulate Ca²⁺ microdomains, set the threshold for Ca²⁺-induced toxicity and participate in local ATP production.

Keywords: aequorin, intracellular calcium concentration, mitochondria, *N*-methyl-D-aspartate, vinblastine. *J. Neurochem.* (2003) **87**, 85–94.

Mitochondria have a large capacity to take up Ca²⁺ from the cytoplasm (Gunter and Gunter 2001; Thayer *et al.* 2002). Consequently, they act as buffers to shape transient changes in the intracellular Ca²⁺ concentration ([Ca²⁺]_i). In neurons, mitochondria blunt the amplitude and prolong the duration of [Ca²⁺]_i responses evoked by activation of voltage-gated (Friel and Tsien 1994; Werth and Thayer 1994; Babcock *et al.* 1997) and ligand-gated (White and Reynolds 1995; Wang and Thayer 1996; Dedov and Roufogalis 2000) Ca²⁺ channels. Increases in the mitochondrial Ca²⁺ concentration ([Ca²⁺]_{mt}) activate mitochondrial dehydrogenases, coupling the increased metabolic demands indicated by the increase in [Ca²⁺]_i to increased ATP production (McCormack *et al.* 1990). When excessive, a raised [Ca²⁺]_{mt} contributes to opening the permeability transition pore, an early event in both apoptotic and necrotic cell death (Nicholls and Budd 2000). Isolated mitochondria accumulate Ca²⁺ when [Ca²⁺]_i rises above a set point in the range of 0.3–1 μM (Nicholls and Scott 1980), so this organelle contributes preferentially to shaping [Ca²⁺]_i when exposed to large increases in [Ca²⁺]_i. [Ca²⁺]_i can reach 200–300 μM near the mouths of Ca²⁺ channels (Llinas *et al.* 1992). Mitochondria near open Ca²⁺

channels in the endoplasmic reticulum (Rizzuto *et al.* 1993) and plasmalemma (Pivovarov *et al.* 1999; Montero *et al.* 2000) take up more Ca²⁺ than mitochondria distributed throughout the cytoplasm. Thus, proximity to a Ca²⁺ source may influence mitochondrial Ca²⁺ uptake.

Mitochondria are localized within the cytoplasm by the microtubule system (Yaffe 1999). A number of microtubule-

Resubmitted article received June 11, 2003; accepted June 12, 2003.

Address correspondence and reprint requests to S. A. Thayer, Department of Pharmacology, University of Minnesota Medical School, 6–120 Jackson Hall, 321 Church Street SE, Minneapolis, MN 55455–0217, USA. E-mail: thayer@med.umn.edu

¹The present address of Guang Jian Wang is Kosair Children's Hospital Research Institute, Department of Pediatrics, University of Louisville, 570 S. Preston Street, Suite 304C, Louisville, KY 40202, USA.

Abbreviations used: [Ca²⁺]_i, intracellular Ca²⁺ concentration; [Ca²⁺]_{mt}, mitochondrial Ca²⁺ concentration; CPA, cyclopiazonic acid; DMEM, Dulbecco's modified Eagle's medium; DMSO, dimethylsulfoxide; HHSS, HEPES-buffered Hanks' salt solution; EGFP, enhanced green fluorescent protein; EYFP, enhanced yellow fluorescent protein; TMRE, tetramethylrhodamine ethyl ester; PMCA, plasma membrane Ca²⁺-ATPase; SERCA, sarcoplasmic and endoplasmic reticulum Ca²⁺-ATPase; FCCP, carbonyl cyanide p-trifluoromethoxy phenyl hydrazone.

based proteins maintain the cellular distribution of mitochondria, and mutation of these molecules invariably causes mitochondria to redistribute, either to cluster near the nucleus or to aggregate along one side of the cell (Nangaku *et al.* 1994; Smirnova *et al.* 1998). Drugs that destabilize microtubules also cause mitochondria to migrate toward the nucleus (Heggeness *et al.* 1978).

We tested the hypothesis that mitochondria near the plasmalemma preferentially take up NMDA-induced Ca^{2+} loads. The distribution of mitochondria was altered by treatment with the microtubule inhibitor vinblastine, which caused mitochondria to pull away from the plasmalemma and form aggregates. Mitochondrial function and ultrastructure appeared normal following the brief vinblastine treatment protocol used in this study. Following the redistribution of mitochondria, NMDA-evoked increases in $[\text{Ca}^{2+}]_i$ were enhanced and evoked increases in $[\text{Ca}^{2+}]_{mt}$ were inhibited. These results are consistent with the hypothesis that a subset of mitochondria near a Ca^{2+} source preferentially takes up Ca^{2+} and they imply location-dependent roles for mitochondria as sources of ATP, Ca^{2+} buffers and targets for Ca^{2+} -induced toxicity.

Materials and methods

Materials

Coelenterazine *f*, tetramethylrhodamine ethyl ester (TMRE) and indo-5F acetoxyethyl ester were purchased from Molecular Probes (Eugene, OR, USA). *cis*-4-Phosphonomethyl-2-piperidine carboxylic acid (CGS19755) was obtained from Research Biochemical International (Natic, MA, USA). Culture media were purchased from Gibco (Grand Island, NY, USA). All other reagents were purchased from Sigma Chemical Company (St Louis, MO, USA).

Cell culture

Primary cultures of rat hippocampal neurons were prepared as described previously (Wang and Thayer 1996). Fetuses were removed on embryonic day 17 from maternal rats anesthetized with CO_2 and killed by decapitation. Hippocampi were dissected and placed in Ca^{2+} - and Mg^{2+} -free HEPES-buffered Hanks' salt solution (HHSS), pH 7.45. HHSS contained 20 mM HEPES, 137 mM NaCl, 1.3 mM CaCl_2 , 0.4 mM MgSO_4 , 0.5 mM MgCl_2 , 5.0 mM KCl, 0.4 mM KH_2PO_4 , 0.6 mM Na_2HPO_4 , 3.0 mM NaHCO_3 and 5.6 mM glucose. Cells were dissociated by trituration through a 5-mL pipette and then a flame-narrowed Pasteur pipette. Cells were pelleted and resuspended in Dulbecco's modified Eagle's medium (DMEM) without glutamine, supplemented with 10% fetal bovine serum (Sigma) and penicillin/streptomycin (100 U/mL and 100 $\mu\text{g}/\text{mL}$ respectively). Dissociated cells were then plated at a density of 50 000 cells per well on to 25-mm round coverglasses (#1) that had been coated with poly-D-lysine (0.1 mg/mL) and washed with H_2O . The neurons were grown in a humidified atmosphere of 10% CO_2 -90% air, pH 7.4, at 37°C, and fed every 7 days by exchange of 75% of the media with DMEM supplemented with 10% horse serum (Gibco) and penicillin/streptomycin. Cells were used after 11 days in culture.

Expression of mitochondrially targeted fluorescent proteins

Enhanced green fluorescent protein (EGFP) (pEGFP-C1) and mitochondrially targeted enhanced yellow fluorescent protein (mtEYFP) (pEYFP-mito) constructs were purchased from Clontech (Palo Alto, CA, USA). A plasmid (pEGFP-mito) that targeted EGFP to the mitochondrion (mtEGFP) was constructed by fusing the mitochondrial targeting sequence of cytochrome *c* oxidase subunit VIII to the 5' end of the *EGFP-N1* gene as described previously (Rizzuto *et al.* 1995; Lakshminpathy and Campbell 1999). All expression vectors used in this study contained the cytomegalovirus promoter.

Hippocampal neurons were transfected with plasmid DNA using the calcium phosphate procedure described by Xia *et al.* (1996), with some modifications. Briefly, 11–14 days after seeding, hippocampal neurons were transferred into serum-free DMEM (2 mL per well, six-well plate) supplemented with 1 mM sodium kynureate, 10 mM MgCl_2 and 5 mM HEPES, pH 7.5, for 15 min. The conditioned medium was saved. A DNA/calcium phosphate precipitate for one six-well plate was prepared by mixing 500 μL 250 mM CaCl_2 and 15 μL plasmid DNA (about 1 $\mu\text{g}/\mu\text{L}$) with an equal volume of 2 \times HEPES-buffered salt solution (274 mM NaCl, 10 mM KCl, 1.4 mM Na_2HPO_4 , 15 mM D-glucose, 42 mM HEPES, pH 7.07). The precipitate was allowed to form for 25–30 min at room temperature (22 °C) before addition to the cultures. One hundred and twenty-five microliters of the DNA/calcium phosphate precipitate were added dropwise to each well and mixed gently. Plates were then returned to the 10% CO_2 incubator. After 20–25 min the incubation was stopped by washing cells three times with 3 mL DMEM per well. The saved conditioned medium was added back to each well, and the cells were returned to a 10% CO_2 incubator at 37°C. The number of transfected neurons ranged from seven to 64 per coverslip with a mean of 25 ± 15 (results of five experiments performed on five platings).

Confocal microscopy

After 24–48 h, transfected neurons were removed from growth media, transferred to a chamber containing HHSS, and viewed through a 60 \times objective. Neurons were imaged with an Olympus Fluoview 300 laser scanning confocal microscope (Melville, NY, USA). Optimal images were obtained by averaging four scans using Kalman filtering. The excitation and emission wavelengths for EGFP were 488 nm, and 522 nm (16nm bandpass), respectively.

$[\text{Ca}^{2+}]_i$ measurement

$[\text{Ca}^{2+}]_i$ was determined with a dual-emission microfluorimeter (Wang and Thayer 2002) to monitor the Ca^{2+} -sensitive fluorescent chelator Indo-5F. Some 24–48 h after transfection, cells were treated with either 1 $\mu\text{g}/\text{mL}$ vinblastine or vehicle [0.1% dimethylsulfoxide (DMSO); untreated] in the culture media at 37°C for 2–3 h. During the last 30–45 min of the incubation, the medium was exchanged for HHSS containing 0.5% bovine serum albumin, 2 μM indo-5F acetoxyethyl ester and either vinblastine or vehicle (untreated). Cells were then placed in a flow-through chamber (Thayer *et al.* 1988) mounted on an inverted microscope. Cells were superfused with HHSS at a rate of 1–2 mL/min for 15 min before starting an experiment. Individual neurons from untreated coverslips (normal mitochondrial distribution) or from vinblastine-treated coverslips (aggregated mitochondria) were identified (70 \times) by EGFP fluorescence [excitation 480(10) nm, emission 540(25) nm] and chosen for $[\text{Ca}^{2+}]_i$ recordings.

After completion of each experiment, the microscope stage was adjusted so that no cells or debris occupied the field of view defined by the diaphragm, and the background light levels were determined (typically <5% of cell counts). Autofluorescence from cells that were not loaded with dye was undetectable. Records were later corrected for background and converted to $[Ca^{2+}]_i$ by the equation $[Ca^{2+}]_i = K_d\beta(R - R_{min})/(R_{max} - R)$, in which R is the 405/495-nm fluorescence ratio. The dissociation constant (K_d) used for Indo-5F was 473 nm, and β was the ratio of emitted fluorescence at 495 nm in the absence and presence of calcium. R_{min} , R_{max} and β were determined in ionomycin-permeabilized cells in calcium-free (1 mM EGTA) and 5 mM Ca^{2+} buffers. Values of R_{min} , R_{max} and β for Indo-5F were 0.21, 1.64 and 4.5 respectively.

$[Ca^{2+}]_{mt}$ measurement

$[Ca^{2+}]_{mt}$ was measured from a population of hippocampal neurons using the Ca^{2+} -sensitive photoprotein aequorin targeted to the mitochondrion, as described previously (Cobbold and Lee 1991; Rizzuto *et al.* 1993; Padua *et al.* 1998). The apo-aequorin gene fused to the mitochondrial targeting sequence from subunit VIII of cytochrome *c* oxidase (COXVIII) was excised from plasmid mtAeq-pMT2 (Rizzuto *et al.* 1993). The gene was inserted into shuttle plasmid pAdRSV4 behind the Rous Sarcoma Virus promoter (Bohn *et al.* 1999). The Gene Transfer Vector Core at the University of Iowa then incorporated the RSVmtAeq expression cassette into a recombinant adenovirus.

After 11–15 days in culture, hippocampal neurons were infected with adenovirus carrying the mitochondrial apo-aequorin expression construct by adding 0.3×10^{10} – 1×10^{10} viral particles to each culture well in 1.5 mL medium and incubated at 37°C. After 24 h, the infection medium was removed and the cells were returned to their original growth medium for 18–24 h. The apo-aequorin protein was reconstituted to form aequorin by incubating transfected cells in serum-free DMEM containing 5 μ M coelenterazine *f* at 37°C for 1–1.5 h before the experiment.

The custom-built luminescence detection system employed here has been described previously (Padua *et al.* 1998). After the apo-aequorin protein had been reconstituted to aequorin, a coverslip with attached neurons was mounted in a stainless steel perfusion chamber and raised to within 10 mm of an inverted photomultiplier tube (Thorn Instruments Rockaway, NJ, USA). The cells were superfused with HHSS for at least 10 min before starting the experiment to wash out any excess coelenterazine. Luminescence was quantified with a Thorn EMI CT 1 counting board installed in a microcomputer sampling at 1 Hz.

Upon binding Ca^{2+} , aequorin emits a photon and its coelenterazine prosthetic group is oxidized, rendering the aequorin incapable of further luminescent reactions with Ca^{2+} . Thus, increasing Ca^{2+} levels will increase the rate of aequorin decay. To correct for the consumption of aequorin, neurons were lysed at the end of the experiment in the presence of 12.6 mM Ca^{2+} in order to discharge any remaining aequorin. Total aequorin counts available during the experiment were determined by integrating photon counts over the entire experiment including lysis. This enabled calculating the fractional rate of aequorin decay (α) from the equation $\alpha = (\text{photon counts per second})/\text{counts remaining}$. The $-\log \alpha$ is proportional to $\log [Ca^{2+}]_{mt}$ and was used to report changes in $[Ca^{2+}]_{mt}$, although the indicator was not calibrated for absolute values of $[Ca^{2+}]_{mt}$.

$[Ca^{2+}]_{mt}$ recordings were filtered digitally with a three-point moving average and peak $[Ca^{2+}]_{mt}$ was determined from the maximum of the filtered trace.

Intramitochondrial pH measurement

Mitochondrial matrix pH was measured in cells expressing pH-sensitive mtEYFP. Acidification of the mitochondrial matrix decreased mtEYFP fluorescence (Llopis *et al.* 1998). mtEYFP fluorescence images [excitation 480(40) nm, emission 535(50) nm] were projected on to a cooled charge-coupled device camera controlled by a computer using Imaging Workbench software (Axon Instruments, Foster City, CA, USA). Images were collected every 10 s and the exposure to excitation light was <50 ms per image.

Measurement of mitochondrial membrane potential

Hippocampal neurons were incubated with 100 nM TMRE for the last 30 min of a 2–3-h treatment with either vehicle or vinblastine (1 μ g/mL) (Schinder *et al.* 1996). TMRE is a cationic fluorescent dye that distributes across membranes in a voltage-dependent manner. Neurons were imaged with an Olympus Fluoview 300 confocal laser scanning microscope using a HeNe laser to excite at 543 nm; emission was detected at >605 nm. Four scans from a single *x-y* plane were averaged using Kalman filtering. Membrane potential was calculated from the ratio of the fluorescent intensity from mitochondria (F_{mt}) relative to cytoplasmic fluorescence (Delcamp *et al.* 1998). As there are no mitochondria in the nucleus, nuclear fluorescence (F_{nuc}) was taken to represent free dye in the cytoplasm. Fluorescent intensities from five to 10 mitochondrial and three nuclear regions were averaged from each cell and converted to membrane potential using the Nernst equation: $V_m = -(RT/zF) \times \ln(F_{mt}/F_{nuc})$, where $RT/zF = 0.0267$.

Electron microscopy

Electron microscopy of cultured hippocampal neurons was carried out using a protocol described by Withers and Banker (1998) with some modifications. Briefly, cells grown on coverslips were fixed with 3.5% glutaraldehyde in culture media for 2 h, rinsed with 0.1 M phosphate buffer, and postfixed in 1% OsO₄ for 30 min. Cells were then rinsed with distilled H₂O, and stained in 5% aqueous uranyl acetate for 1 h. After washing with distilled H₂O, cells were dehydrated with successive concentrations of ethanol, then embedded in Epon resin. Ultrathin sections were cut and poststained with 4% uranyl acetate for 20 min followed by modified Reynold's lead stain for 3 min. Sections were examined in a JOEL 1200 EX electron microscope (Peabody, MA, USA).

Statistical analysis

Data are presented as Mean \pm S.E.M. Statistical comparisons were made by Student's *t*-test.

Results

Disruption of the microtubule system alters mitochondrial localization

Mitochondria were visualized in live hippocampal neurons in culture using confocal imaging of mitochondrially targeted

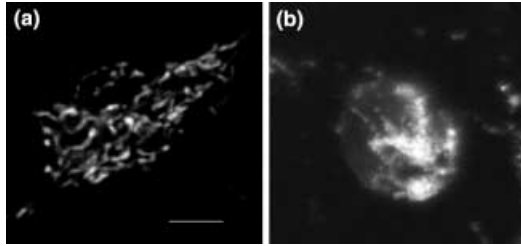


Fig. 1 Mitochondria redistribute after disruption of the microtubule system. Rat hippocampal neurons were transfected with pEGFP-mito after 11–14 days in culture. (a) 24–48 h after transfection extensive vermiform mitochondria were visualized throughout the soma. (b) 2–3 h after the addition of vinblastine (1 $\mu\text{g}/\text{mL}$) to the culture media the soma became rounded and mitochondria aggregated. Untreated cells were exposed to an equal volume of drug vehicle (DMSO). The images shown are single confocal sections and are representative of at least four separate experiments. Scale bar is 5 μm and applies to both images.

EGFP (mtEGFP). Extensive vermiform structures were distributed throughout the cytoplasm, consistent with previously reported mitochondrial morphology (Fig. 1a) (Rizzuto *et al.* 1998). The nucleoplasm, the nuclear envelope and the plasmalemma were devoid of fluorescence. Discrete, individual mitochondria were seen in neuronal processes. Owing to the high density of mitochondria within the soma we could not determine whether the fluorescence represented a syncytial organelle of an extended reticular network or many intermingled individual mitochondria.

We next altered the distribution of mitochondria by treating the cells with the microtubule inhibitor vinblastine. Treatment of hippocampal neurons with 1 $\mu\text{g}/\text{mL}$ vinblastine for 2–3 h caused mitochondria to aggregate (Fig. 1b). The initial widely distributed fluorescence seen before drug treatment (Fig. 1a) changed to sites of intense signal, often adjacent to the nucleus, with other regions of the cell completely devoid of fluorescence. A rounding of the soma was observed after 2–3 h of treatment with vinblastine in some cells, an effect that became pronounced after 24 h. These observations are consistent with vinblastine disrupting the microtubule system, resulting in the redistribution of mitochondria. Mitochondrial aggregation, defined by the presence of aggregated masses within the soma and the absence of discrete vermiform structures, was seen in $81 \pm 16\%$ of neurons treated with vinblastine for 2–3 h ($n = 8$ coverslips for a total of 177 transfected cells).

$[\text{Ca}^{2+}]_i$ regulation is altered in vinblastine-treated cells
NMDA-induced $[\text{Ca}^{2+}]_i$ responses were examined in untreated cells and cells with altered mitochondrial distribution. Cells were transfected with pEGFP-mito and 24–48 h later treated with either vinblastine (1 $\mu\text{g}/\text{mL}$) or vehicle for 2–3 h. Cells were loaded with the low-affinity Ca^{2+} indicator Indo-5F acetoxymethyl ester during the last 30–45 min of treatment.

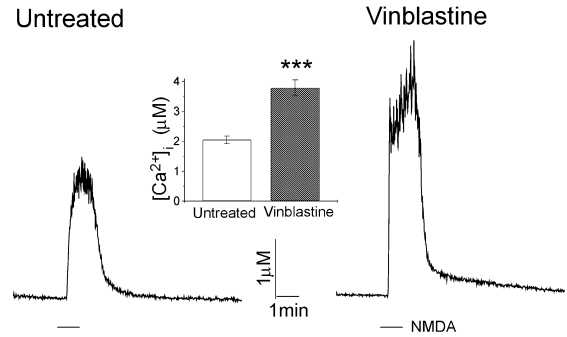


Fig. 2 NMDA-evoked $[\text{Ca}^{2+}]_i$ increases are larger in vinblastine-treated cells. Neurons were transfected with pEGFP-mito, exposed to either vehicle (0.1% DMSO; untreated) or vinblastine (1 $\mu\text{g}/\text{mL}$), and loaded with Indo-5F acetoxymethyl ester. Individual cells with a normal mitochondrial distribution (untreated) or aggregated mitochondria (vinblastine) were identified and $[\text{Ca}^{2+}]_i$ recorded. NMDA (200 μM) was applied at the times indicated by the horizontal bars. Traces are representative of 26–27 cells from at least 10 cultures as summarized in the bar graph. $***p < 0.001$ versus untreated.

The distribution of mitochondria was confirmed to be normal before making recordings from untreated cells (see Fig. 1a). For vinblastine-treated cultures, recordings were made only from cells with aggregated mitochondria (see Fig. 1b). Basal $[\text{Ca}^{2+}]_i$ levels were raised slightly in vinblastine-treated cells (158 ± 16 nM; $n = 27$) relative to levels in untreated cells (127 ± 10 nM; $n = 26$) ($p < 0.05$) (Fig. 2). Stimulation with 200 μM NMDA (1 min) elicited a significantly greater $[\text{Ca}^{2+}]_i$ increase in vinblastine-treated (3779 ± 265 nM; $n = 11$) than untreated cells (2047 ± 129 nM; $n = 10$) ($p < 0.0001$) (Fig. 2). These data are consistent with the idea that movement of mitochondria away from the source of Ca^{2+} influx at the plasma membrane reduces mitochondrial exposure to high $[\text{Ca}^{2+}]_i$ near the mouth of plasmalemma Ca^{2+} channels resulting in a reduction in Ca^{2+} uptake.

If reduced mitochondrial Ca^{2+} uptake is responsible for the increased amplitude of the NMDA-induced $[\text{Ca}^{2+}]_i$ response in vinblastine-treated cells, then $[\text{Ca}^{2+}]_{\text{mt}}$ should be reduced in these cells. We measured $[\text{Ca}^{2+}]_{\text{mt}}$ directly using the Ca^{2+} -sensitive photoprotein aequorin targeted to the mitochondrion. The mitochondrially targeted apo-aequorin gene was transferred to hippocampal neurons using an adenoviral vector as described previously (Wang and Thayer 2002). The NMDA-induced intramitochondrial Ca^{2+} response was significantly smaller in vinblastine-treated cells (0.35 ± 0.03 $-\log \alpha$; $n = 7$) than that in untreated cells (0.65 ± 0.04 $-\log \alpha$; $n = 6$) ($p < 0.01$) (Fig. 3). The rapid decay of the $[\text{Ca}^{2+}]_{\text{mt}}$ response was due to consumption of aequorin which emits one photon per molecule irreversibly upon binding Ca^{2+} . Mitochondria in vinblastine-treated cells sequestered less Ca^{2+} than those in untreated cells, consistent with the corresponding increase in the amplitude of the NMDA-induced $[\text{Ca}^{2+}]_i$ response in these cells.

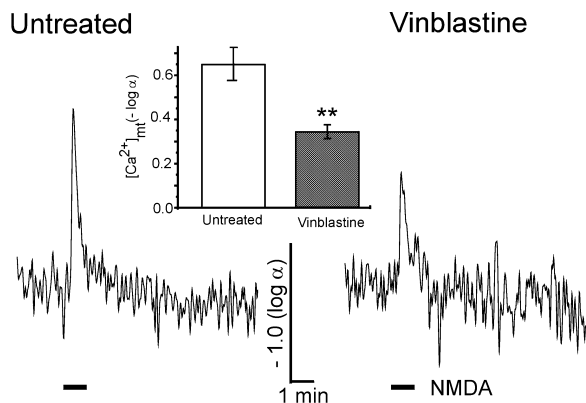


Fig. 3 Mitochondrial uptake of NMDA-induced Ca^{2+} influx is reduced in vinblastine-treated cells. Hippocampal cultures were exposed to adenovirus harboring the mitochondrially targeted apo-aequorin gene 24 h before measuring $[Ca^{2+}]_{mt}$. The culture was treated with either vehicle (0.1% DMSO; untreated) or 1 μ g/mL vinblastine for 2–3 h before recording. Apo-aequorin was reconstituted with its cofactor coelenterazine *f* 1 h before recording. $[Ca^{2+}]_{mt}$ was recorded from a population of cells expressing mitochondrially targeted aequorin using a flow-through luminometer (Padua *et al.* 1998). $[Ca^{2+}]_{mt}$ is expressed as $-\log \alpha$ which is proportional to $\log [Ca^{2+}]$ (Cobbold and Lee 1991; Rizzuto *et al.* 1993; Padua *et al.* 1998). Traces are representative of six to seven recordings from three platings. NMDA (200 μ M) was applied at the times indicated by the horizontal bars. $**p < 0.01$ versus untreated.

Vinblastine alters the distribution but not the function or ultrastructure of mitochondria

Prolonged exposure (24 h) to 1 μ g/mL vinblastine is toxic to hippocampal neurons. It was therefore important to determine the effects of the 2–3-h treatment used here on mitochondrial structure and function. Several lines of evidence suggested that mitochondrial function was not impaired following a 2–3-h exposure to vinblastine. Respiring mitochondria maintain a proton gradient across the inner membrane. We therefore determined the effects of vinblastine on matrix pH and the membrane potential across the inner mitochondrial membrane.

In order to assess the effect of vinblastine on matrix pH we expressed mtEYFP, which fluoresces more strongly at alkaline than at neutral pH (Llopis *et al.* 1998) (Fig. 4a). Vinblastine-treated cells displayed aggregated fluorescence (Fig. 4b). However, both untreated and vinblastine-treated cells showed a comparable degree of quenching produced by the protonophore carbonyl cyanide p-trifluomethoxy phenyl hydrazone (FCCP), which dissipates the mitochondrial pH gradient (Figs 4c and d). Exposure to 10 μ M FCCP for 3 min decreased mtEYFP fluorescence by $11 \pm 1\%$ ($n = 12$) (Fig. 4c) in untreated neurons and by $10 \pm 1\%$ ($n = 11$) (Fig. 4d) in vinblastine-treated cells (Fig. 4e) ($p > 0.05$).

We measured mitochondrial membrane potential with the cationic fluorescent dye TMRE, which distributes across membranes in a voltage-dependent manner (Nicholls and

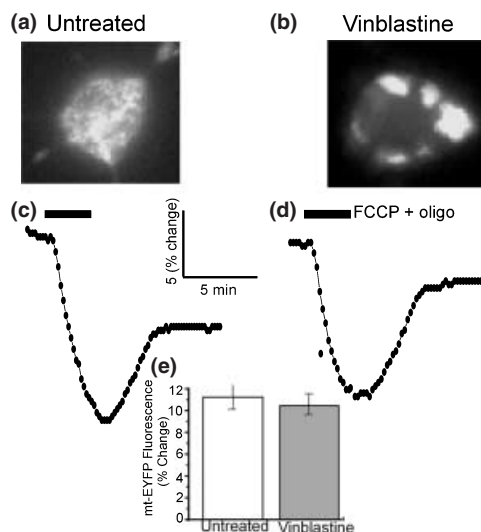


Fig. 4 Vinblastine does not affect the pH gradient across the mitochondrial inner membrane. Hippocampal neurons were transfected with pEYFP-mito and 24–48 h later treated with either vehicle or 1 μ g/mL vinblastine for 2–3 h. Cells with normally distributed mitochondria (untreated) and aggregated mitochondria (vinblastine) were identified, and fluorescence intensity quantified using digital imaging. Fluorescence intensities were normalized to initial intensity (before FCCP treatment), and plotted against time. FCCP (10 μ M) and oligomycin (oligo; 1 μ M) were applied at the times indicated by the horizontal bars. Bar graph summarizes data from 11–12 cells recorded from at least three cell cultures.

Ward 2000). Confocal images of untreated and vinblastine-treated cells in the presence of 100 nM TMRE are shown in Figs 5(a) and (b) respectively. Strong TMRE fluorescence was detected as worm-like structures in untreated cells and as aggregates in vinblastine-treated cells. We calculated the membrane potential from the ratio of the fluorescence intensity from the presumed mitochondrial structures to the intensity of the nucleus that is void of mitochondria. Mitochondrial membrane potentials calculated from the Nernst equation were -129 ± 7 mV for untreated and -137 ± 12 mV for vinblastine-treated cells (Fig. 5c). TMRE accumulation into mitochondria was dependent on mitochondrial membrane potential as indicated by the loss of signal after treatment with the mitochondrial uncoupling agent FCCP (data not shown).

Protein import into the mitochondrion requires an electrochemical gradient across the inner membrane (Schatz and Dobberstein 1996). We treated hippocampal neurons with vinblastine (1 μ g/mL, 2–3 h) before transfection with pEGFP-mito. Fluorescence labeling was detected within subcellular structures in these cells 24–48 h later, indicating that sufficient membrane potential was maintained to enable protein import ($n = 4$ coverslips; data not shown).

To ascertain whether vinblastine produced structural injury to mitochondria in hippocampal neurons we examined the

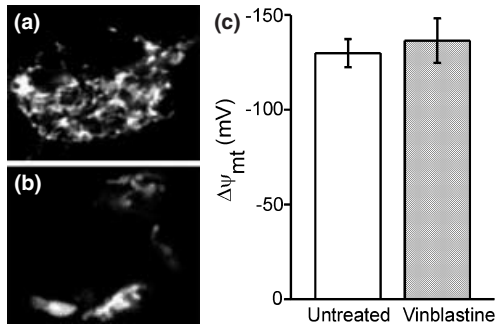


Fig. 5 Vinblastine does not affect the mitochondrial membrane potential. Hippocampal neurons were treated with either vehicle (a) or 1 $\mu\text{g}/\text{mL}$ vinblastine (b) for 2–3 h. Cells were bathed in 100 nM TMRE during the last 30 min of treatment and imaged with a confocal microscope. Representative images are from a single x - y plane. (c) Fluorescence intensities within vermiform mitochondria (a) or aggregated mitochondria (b) were divided by the cytoplasmic intensity measured in the nucleus of the same cell and input to the Nernst equation to calculate membrane potential. Bar graph summarizes mitochondrial membrane potential ($\Delta\Psi_{mt}$) from ≥ 13 cells per group from at least two cell cultures.

ultrastructure of mitochondria in vinblastine-treated cells using electron microscopy. Figure 6 shows electron micrographs from untreated and vinblastine-treated cells; mitochondria in both cells had structurally intact inner and outer membranes with well defined cristae. Consistent with our confocal observations (Fig. 1), mitochondria in untreated hippocampal neurons were distributed throughout the cytoplasm whereas those in vinblastine-treated cells were aggregated on one side of the cell (bottom right side in Fig. 6b) leaving other parts of the cell almost completely devoid of mitochondria. Scattered bundles of microtubules were seen in vinblastine-treated cells, but not in control cells, confirming that these cells had been affected by the vinblastine (Muller *et al.* 1988). In summary, vinblastine appears to alter the distribution of mitochondria without significantly affecting mitochondrial energy status or structure.

Specificity of vinblastine effects on neuronal Ca^{2+} homeostasis

To further address the specificity of the vinblastine effect to the mitochondrially mediated component of Ca^{2+} homeostasis we examined additional Ca^{2+} -regulated responses in vinblastine-treated cells. Small action potential-induced increases in $[\text{Ca}^{2+}]_i$ recover by a mono-exponential process that is predominantly dependent on the plasma membrane Ca^{2+} -ATPase (PMCA) (Werth *et al.* 1996; Usachev *et al.* 2002). $[\text{Ca}^{2+}]_i$ recovery following a brief train of action potentials (1 s, 10 Hz) was similar in untreated ($\tau = 3.3 \pm 0.2$ s; $n = 7$) and vinblastine-treated ($\tau = 2.9 \pm 0.2$ s; $n = 5$) hippocampal neurons (Figs 7a and c). These data suggest that vinblastine treatment did not deprive the

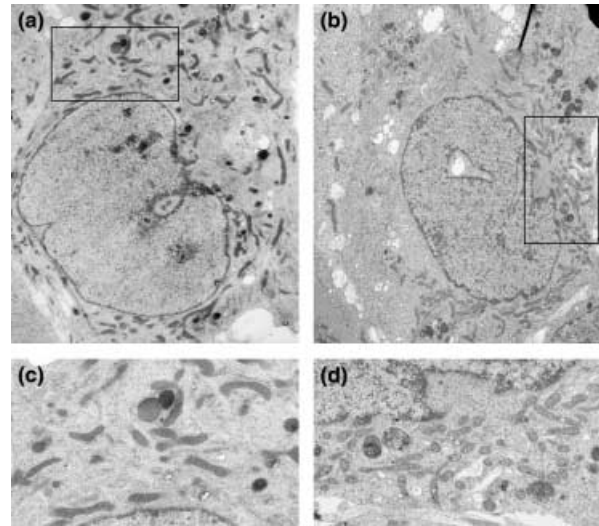


Fig. 6 Vinblastine treatment changes the distribution, but not the ultrastructure, of mitochondria in hippocampal neurons. Electron micrographs show an untreated cell (a) and a cell treated with 1 $\mu\text{g}/\text{mL}$ vinblastine (b) for 2–3 h ($\times 5000$). Mitochondria were distributed throughout the untreated cell but were clustered near the bottom right corner of the vinblastine-treated cell. Thick bundles of microtubules were seen in the vinblastine-treated cell. (c, d) Higher magnification ($\times 10\,000$) of boxed regions. Micrographs are representative of six to seven cells.

PMCA of ATP nor did drug-induced swelling alter the function of the plasmalemmal Ca^{2+} pump.

We also examined the effects of vinblastine on responses evoked by 10 μM NMDA. In contrast to the large increase in Ca^{2+} evoked by 200 μM NMDA, the response to a low concentration was minimally affected by mitochondrial Ca^{2+} uptake (Wang and Thayer 2002). Thus, the peak amplitude of the response evoked by 10 μM NMDA is predominantly determined by Ca^{2+} influx. As shown in Figs 7(b) and (d), treatment with vinblastine did not affect the amplitude of the response elicited by 10 μM NMDA. The peak $[\text{Ca}^{2+}]_i$ increase was 673 ± 51 nM ($n = 21$) in untreated and 688 ± 85 nM ($n = 14$) in vinblastine-treated cells. These data suggest that Ca^{2+} influx pathways activated by NMDA are not affected by vinblastine treatment.

To determine the role of endoplasmic reticulum Ca^{2+} stores on the NMDA response, we compared the amplitude of responses evoked by 200 μM NMDA in the absence and presence of 5 μM cyclopiazonic acid (CPA) (Fig. 8a). CPA inhibits sarcoplasmic and endoplasmic reticulum Ca^{2+} -ATPases (SERCAs), and so inhibits Ca^{2+} uptake into the endoplasmic reticulum and allows stored Ca^{2+} to leak into the cytoplasm. Application of CPA produced a small, transient increase in $[\text{Ca}^{2+}]_i$ (89 ± 7 nM; $n = 27$) consistent with depletion of Ca^{2+} stores (recording not shown). CPA increased the amplitude of the NMDA-evoked response in control cells to a peak $[\text{Ca}^{2+}]_i$ of 2884 ± 375 nM ($n = 14$),

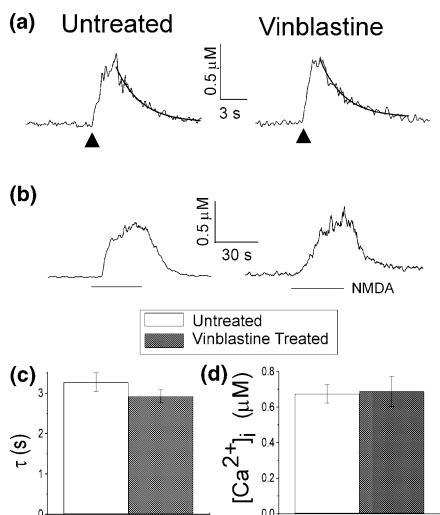


Fig. 7 Vinblastine does not affect PMCA-mediated Ca^{2+} efflux or NMDA-evoked Ca^{2+} influx. Hippocampal neurons were treated for 2–3 h with vehicle (untreated) or vinblastine (1 μ g/mL). (a) Brief trains of action potentials were evoked by electric field stimulation (1 s, 10 Hz) at the times indicated (\blacktriangle). $[Ca^{2+}]_i$ recovered by a monoexponential process in untreated and vinblastine-treated cells. Exponential fits to the data are displayed as solid lines. Traces are representative of at least five experiments. (b) Cells were superfused with Mg^{2+} -free medium containing 10 μ M glycine and 1 μ M tetrodotoxin and then stimulated with 10 μ M NMDA (30 s) at the times indicated by the horizontal bars. Traces are representative of at least 14 experiments. (c) The bar graph displays the mean time constants (τ) for $[Ca^{2+}]_i$ recovery kinetics following a train of action potentials in untreated (open bar) and vinblastine-treated (solid bar) cells ($p > 0.05$). (d) The bar graph displays the amplitude of $[Ca^{2+}]_i$ increases evoked by 10 μ M NMDA from untreated and vinblastine-treated cells ($p > 0.05$).

consistent with the loss of SERCA-mediated Ca^{2+} uptake. The amplitude of the NMDA-evoked response in cells treated with vinblastine and CPA was 4198 ± 577 nM ($n = 15$), a significant increase above that seen in cells treated with CPA alone ($p < 0.05$). Because treatment with CPA did not occlude the enhancement produced by treatment with vinblastine, we conclude that the increase in the amplitude of the NMDA-evoked response was primarily due to effects on mitochondria rather than endoplasmic reticulum.

The microtubule-stabilizing agent paclitaxel has been reported to open the mitochondrial permeability transition pore (Kidd *et al.* 2002). Although vinblastine, the microtubule-destabilizing agent used here, would be predicted to have an opposite effect, if any, we thought it prudent to address this issue. The paclitaxel-induced opening of the permeability transition pore was blocked by 5 μ M cyclosporine A (Kidd *et al.* 2002). As shown in Fig. 8(b), pretreatment with 5 μ M cyclosporine for 10 min increased the amplitude of the NMDA-evoked response in control cells to a peak $[Ca^{2+}]_i$ of 2710 ± 457 nM ($n = 13$). This increase in amplitude prob-

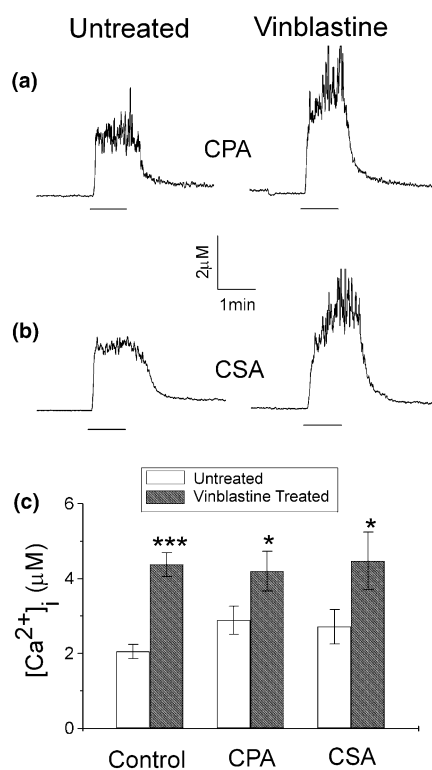


Fig. 8 Vinblastine does not affect Ca^{2+} stores or the mitochondrial permeability transition pore. Hippocampal neurons were treated for 2 h with vehicle (untreated) or vinblastine (1 μ g/mL). (a, b) 200 μ M NMDA was applied at the times indicated by the horizontal bars. (a) The NMDA-evoked response in cells treated with CPA plus vinblastine (right) was significantly greater than the response elicited from cells treated with CPA alone (left). (b) Cyclosporine A (CSA; 5 μ M) did not prevent the enhanced NMDA-evoked response in vinblastine-treated cells. (c) The bar graph displays the amplitude of NMDA-induced increases in $[Ca^{2+}]_i$ from untreated and vinblastine-treated cells. Control values were derived from a subset of the experiments summarized in Fig. 2, and include only those recordings performed on the same day as the CPA and CSA experiments. *** $p < 0.0001$, * $p < 0.05$ versus untreated.

ably results from increased Ca^{2+} influx via the NMDA receptor owing to cyclosporine A-dependent relief from the tonic inhibition of the NMDA receptor by the phosphatase calcineurin (Lieberman and Mody 1994). The amplitude of the NMDA-evoked response in cells treated with vinblastine and cyclosporine A was 4475 ± 767 nM ($n = 15$), a significant increase above that seen in cells treated with cyclosporine A alone ($p < 0.05$). As treatment with cyclosporine A did not prevent the enhancement produced by treatment with vinblastine, we conclude that the increase in the amplitude of the NMDA-evoked response was not due to an effect of vinblastine on the permeability transition pore. This observation is also consistent with our electron microscopic results, which showed that the mitochondrial ultrastructure was not altered by treatment with vinblastine.

Discussion

We have shown that pharmacological disruption of microtubules produces mitochondrial aggregates and increases the amplitude of NMDA-induced $[Ca^{2+}]_i$ responses. We suggest that Ca^{2+} uptake by mitochondria was reduced because mitochondria that would have taken up large amounts of Ca^{2+} owing to exposure to high $[Ca^{2+}]_i$ near plasmalemmal Ca^{2+} channels were removed from this advantageous location. These results lend support to the emerging view that mitochondria significantly shape transient increases in $[Ca^{2+}]_i$ close to the Ca^{2+} source and therefore play a major role in regulating processes that are triggered by large local increases in $[Ca^{2+}]_i$ (Rizzuto *et al.* 2000; Montero *et al.* 2001). Other support for this hypothesis comes from observations following activation of voltage-gated Ca^{2+} channels that demonstrate $[Ca^{2+}]_i$ in excess of 200 μM near the mouth of the channel (Llinas *et al.* 1992), large increases in $[Ca^{2+}]_{mt}$ in a subset of mitochondria (Montero *et al.* 2000), and electron probe microanalysis showing that mitochondrial Ca^{2+} deposits formed a radial spread (Pivovarova *et al.* 1999).

We have concluded that the altered distribution of mitochondria accounts for the increased amplitude of NMDA-induced $[Ca^{2+}]_i$ responses in vinblastine-treated cells. However, alternative explanations were also considered. An increase in Ca^{2+} influx seems unlikely because the $[Ca^{2+}]_{mt}$ response was actually reduced. Furthermore, the amplitude of small increases in $[Ca^{2+}]_i$ evoked by 10 μM NMDA, responses with relatively minor mitochondrial Ca^{2+} buffering (Werth *et al.* 1996; Usachev *et al.* 2002; Wang and Thayer 2002), were not affected by treatment with vinblastine, suggesting that vinblastine did not increase Ca^{2+} influx via NMDA and voltage-gated Ca^{2+} channels. In other studies, poisoning mitochondria actually decreased Ca^{2+} influx owing to increased Ca^{2+} -mediated feedback inhibition resulting from reduced Ca^{2+} buffering near the mouth of the channel (Budd and Nicholls 1996; Hoth *et al.* 2000). Impaired Ca^{2+} efflux might also increase the amplitude of the NMDA-induced $[Ca^{2+}]_i$ response. However, recovery from action potential-induced Ca^{2+} loads was not affected by vinblastine. Recovery from these small Ca^{2+} loads is predominantly mediated by the plasma membrane Ca^{2+} pump (Werth *et al.* 1996; Usachev *et al.* 2002). Thus, these data also support our contention that treatment with vinblastine does not affect the ATP/ADP ratio. Disruption of microtubules might affect the endoplasmic reticulum; however, preventing Ca^{2+} uptake into the endoplasmic reticulum did not prevent the increase in the amplitude of the $[Ca^{2+}]_i$ response evoked by 200 μM NMDA in vinblastine-treated cells. In summary, the increased amplitude of the $[Ca^{2+}]_i$ increase evoked by 200 μM NMDA most probably results from altered mitochondrial Ca^{2+} buffering.

Interpretation of this study is complicated by the possibility that mitochondrial function was impaired by vinblastine

treatment, raising the concern that the increased amplitude of the NMDA-evoked $[Ca^{2+}]_i$ response results from the reduced potential for mitochondria to take up Ca^{2+} as opposed to their redistribution. Several lines of evidence suggest that mitochondrial function was not impaired. Direct measurement of the mitochondrial membrane potential with TMRE revealed physiological voltages across the inner membrane that were similar for untreated and vinblastine-treated cells. Other mitochondrial functions that require an electrochemical gradient across the inner mitochondrial membrane were also normal, including ultrastructure, the pH gradient and the ability to import cytoplasmic proteins. Additionally, there is precedent in the literature for maintained function of mitochondria following redistribution. Herpes virus infection results in migration of mitochondria towards the nucleus; these perinuclear mitochondria maintained their membrane potential for at least 6 h (Murata *et al.* 2000). However, there are also reports that altering the cytoskeleton will affect mitochondrial function (Rappaport *et al.* 1998). Of particular relevance to this study are reports that mitochondrial association with microtubules affects the opening of the permeability transition pore. This was shown most clearly for the microtubule-stabilizing agent paclitaxel, which held the permeability transition pore in the open state (Kidd *et al.* 2002). In our experiments with hippocampal neurons we did not observe a large increase in basal $[Ca^{2+}]_i$, as was seen when paclitaxel was applied to pancreatic acinar cells (Kidd *et al.* 2002), suggesting that microtubule-stabilizing agents have more significant effects on the permeability transition pore than microtubule-destabilizing agents. Colchicine also affected the permeability phase transition at high concentrations (Evtodienko *et al.* 1996). The failure of cyclosporine A, which inhibits opening of the permeability transition pore, to inhibit the increase in the NMDA-induced $[Ca^{2+}]_i$ response produced by treatment with vinblastine suggests that the permeability transition pore was not opened by either the NMDA stimulus or the vinblastine treatment used in this study. The normal mitochondrial ultrastructure and matrix pH gradient observed in cells treated with 1 $\mu g/mL$ vinblastine for 2 h are also consistent with the suggestion that this concentration and duration of treatment did not affect the permeability transition pore.

Vinblastine and other vinca alkaloids are anti-cancer drugs that arrest cell proliferation by inhibiting the mitotic spindle apparatus. Neurotoxicity is a major and often dose-limiting side-effect of vincristine and vindesine, and to a lesser extent of vinblastine. The mechanism by which these agents cause neurotoxicity is not fully understood. Previous studies have focused on inhibition of neurite outgrowth and axonal transport (Muller *et al.* 1988; Geldof *et al.* 1998). This study suggests that impaired Ca^{2+} buffering might also contribute to neurotoxicity produced by vinca alkaloids.

In Alzheimer's disease and other tauopathy-related neurodegenerative diseases, tau mutations lead to the formation of

neurofibrillary tangles that accumulate in the cytoplasm, destabilize microtubules and disrupt the organization of cellular organelles, including mitochondria (Goedert 1993; Hardy and Gwinn-Hardy 1998). Changes in the distribution of mitochondria may increase vulnerability to insults, such as glutamate neurotoxicity, ischemia and aging. Alternatively, if excessive Ca^{2+} uptake into mitochondria opens the permeability transition pore leading to cytochrome *c* release and activation of the apoptotic cascade (Petronilli *et al.* 2001), then localized Ca^{2+} uptake by mitochondria may increase vulnerability to Ca^{2+} -mediated neurotoxicity. This suggests that a subset of mitochondria near a Ca^{2+} source might initiate apoptosis, even when the average whole-cell $[Ca^{2+}]_i$ is not greatly increased, and raises interesting questions regarding the threshold for triggering apoptosis and neuronal tolerance to Ca^{2+} influx.

The specificity of Ca^{2+} signals is conferred in part by the spatial profile of the change in $[Ca^{2+}]_i$. Ca^{2+} entry by different routes activates distinct signaling pathways (Bading *et al.* 1993; Ghosh and Greenberg 1995). Indeed, Ca^{2+} entry via NMDA-gated channels is toxic whereas comparable Ca^{2+} loads entering via voltage-gated Ca^{2+} channels are not (Sattler *et al.* 1999). Activation of extrasynaptic NMDA receptors depolarizes mitochondria and triggers cell death (Hardingham *et al.* 2002). This source specificity of Ca^{2+} signaling is dependent upon the precise arrangement of intracellular Ca^{2+} -sensing targets such as mitochondria. Because altering the distribution of mitochondria altered the $[Ca^{2+}]_i$ response, we speculate that the converse is also true, namely that mitochondria alter the spatial profile of Ca^{2+} signals. Mitochondrial Ca^{2+} buffering modulates a number of local signaling events, including catecholamine secretion from chromaffin cells (Montero *et al.* 2000), hormone release from gonadotropes (Kaftan *et al.* 2000), short-term plasticity at the crayfish neuromuscular junction (Tang and Zucker 1997), inactivation of voltage-gated and store-operated Ca^{2+} channels (Budd and Nicholls 1996; Hoth *et al.* 2000), and release and refilling of Ca^{2+} stores (Hajnoczky *et al.* 1999; Lewis 2001). Furthermore, these processes all require energy, which could best be met by enhanced ATP production by local mitochondria sensing the Ca^{2+} stimulus, an idea consistent with the high concentration of mitochondria in cellular regions of high-energy demand (Hollenbeck 1996).

Mitochondria participate in and help to create local Ca^{2+} signaling domains. Understanding the components and precise arrangement of these assemblies will provide insight into the factors that shape $[Ca^{2+}]_i$ waveforms and will clarify how $[Ca^{2+}]_i$ signals regulate metabolism and trigger neurotoxicity.

Acknowledgements

We thank Wenna Lin for the preparation of neuronal cultures. The National Institutes of Health (DA07304, DA11806) and the National Science Foundation (IBN0110409) supported this work.

References

- Babcock D. F., Herrington J., Goodwin P. C., Park Y. B. and Hille B. (1997) Mitochondrial participation in the intracellular Ca^{2+} network. *J. Cell Biol.* **136**, 833–844.
- Bading H., Ginty D. D. and Greenberg M. E. (1993) Regulation of gene expression in hippocampal neurons by distinct calcium signaling pathways. *Science* **260**, 181–186.
- Bohn M. C., Choi-Lundberg D. L., Davidson B. L., Leranath C., Kozlowski D. A., Smith J. C., O'Banion M. K. and Redmond D. E. Jr (1999) Adenovirus-mediated transgene expression in nonhuman primate brain. *Hum. Gene Ther.* **10**, 1175–1184.
- Budd S. L. and Nicholls D. G. (1996) A reevaluation of the role of mitochondria in neuronal Ca^{2+} homeostasis. *J. Neurochem.* **66**, 403–411.
- Cobbold P. H. and Lee J. A. C. (1991) Aequorin measurements of cytoplasmic free calcium, in *Cellular Calcium; A Practical Approach* (McCormack J. G. and Cobbold P. H., eds), pp. 55–81. Oxford University Press, New York.
- Dedov V. N. and Roufogalis B. D. (2000) Mitochondrial calcium accumulation following activation of vanilloid (VR1) receptors by capsaicin in dorsal root ganglion neurons. *Neuroscience* **95**, 183–188.
- Delcamp T. J., Dales C., Ralenkotter L., Cole P. S. and Hadley R. W. (1998) Intramitochondrial $[Ca^{2+}]_i$ and membrane potential in ventricular myocytes exposed to anoxia-reoxygenation. *Am. J. Physiol.* **275**, H484–H494.
- Evtodienko Y. V., Teplova V. V., Sidash S. S., Ichas F. and Mazat J. P. (1996) Microtubule-active drugs suppress the closure of the permeability transition pore in tumour mitochondria. *FEBS Lett.* **393**, 86–88.
- Friel D. D. and Tsien R. W. (1994) An FCCP-sensitive Ca^{2+} store in bullfrog sympathetic neurons and its participation in stimulus-evoked changes in $[Ca^{2+}]_i$. *J. Neurosci.* **14**, 4007–4024.
- Geldof A. A., Minneboo A. and Heimans J. J. (1998) Vinca-alkaloid neurotoxicity measured using an *in vitro* model. *J. Neurooncol.* **37**, 109–113.
- Ghosh A. and Greenberg M. E. (1995) Calcium signaling in neurons: molecular mechanisms and cellular consequences. *Science* **268**, 239–247.
- Goedert M. (1993) Tau protein and the neurofibrillary pathology of Alzheimer's disease. *Trends Neurosci.* **16**, 460–465.
- Gunter T. E. and Gunter K. K. (2001) Uptake of calcium by mitochondria: transport and possible function. *IUBMB Life* **52**, 197–204.
- Hajnoczky G., Hager R. and Thomas A. P. (1999) Mitochondria suppress local feedback activation of inositol 1,4,5-trisphosphate receptors by Ca^{2+} . *J. Biol. Chem.* **274**, 14157–14162.
- Hardingham G. E., Fukunaga Y. and Bading H. (2002) Extrasynaptic NMDARs oppose synaptic NMDARs by triggering CREB shut-off and cell death pathways. *Nat. Neurosci.* **5**, 405–414.
- Hardy J. and Gwinn-Hardy K. (1998) Genetic classification of primary neurodegenerative disease. *Science* **282**, 1075–1079.
- Heggeness M. H., Simon M. and Singer S. J. (1978) Association of mitochondria with microtubules in cultured cells. *Proc. Natl Acad. Sci. USA* **75**, 3863–3866.
- Hollenbeck P. J. (1996) The pattern and mechanism of mitochondrial transport in axons. *Front. Biosci.* **1**, d91–d102.
- Hoth M., Button D. C. and Lewis R. S. (2000) Mitochondrial control of calcium-channel gating: a mechanism for sustained signaling and transcriptional activation in T lymphocytes. *Proc. Natl Acad. Sci. USA* **97**, 10607–10612.
- Kaftan E. J., Xu T., Abercrombie R. F. and Hille B. (2000) Mitochondria shape hormonally induced cytoplasmic calcium oscillations and modulate exocytosis. *J. Biol. Chem.* **275**, 25465–25470.
- Kidd J. F., Pilkington M. F., Schell M. J., Fogarty K. E., Skepper J. N., Taylor C. W. and Thorn P. (2002) Paclitaxel affects cytosolic

- calcium signals by opening the mitochondrial permeability transition pore. *J. Biol. Chem.* **277**, 6504–6510.
- Lakshminpathy U. and Campbell C. (1999) The human DNA ligase III gene encodes nuclear and mitochondrial proteins. *Mol. Cell. Biol.* **19**, 3869–3876.
- Lewis R. S. (2001) Calcium signaling mechanisms in T lymphocytes. *Annu. Rev. Immunol.* **19**, 497–521.
- Lieberman D. N. and Mody I. (1994) Regulation of NMDA channel function by endogenous Ca^{2+} -dependent phosphatase. *Nature* **369**, 235–239.
- Llinas R., Sugimori M. and Silver R. B. (1992) Microdomains of high calcium concentration in a presynaptic terminal. *Science* **256**, 677–679.
- Llopis J., McCaffery J. M., Miyawaki A., Farquhar M. G. and Tsien R. Y. (1998) Measurement of cytosolic, mitochondrial, and Golgi pH in single living cells with green fluorescent proteins. *Proc. Natl Acad. Sci. USA* **95**, 6803–6808.
- McCormack J. G., Halestrap A. P. and Denton R. M. (1990) Role of calcium ions in regulation of mammalian intramitochondrial metabolism. *Physiol. Rev.* **70**, 391–425.
- Montero M., Alonso M. T., Carnicero E., Cuchillo-Ibanez I., Albillos A., Garcia A. G., Garcia-Sancho J. and Alvarez J. (2000) Chromaffin-cell stimulation triggers fast millimolar mitochondrial Ca^{2+} transients that modulate secretion. *Nat. Cell Biol.* **2**, 57–61.
- Montero M., Alonso M. T., Albillos A., Cuchillo-Ibanez I., Olivares R., Garcia A. G., Garcia-Sancho J. and Alvarez J. (2001) Control of secretion by mitochondria depends on the size of the local $[\text{Ca}^{2+}]$ after chromaffin cell stimulation. *Eur. J. Neurosci.* **13**, 2247–2254.
- Muller L. J., Moorer-van Delft C. M. and Roubos E. W. (1988) Snail neurons as a possible model for testing neurotoxic side effects of antitumor agents: paracrystal formation by Vinca alkaloids. *Cancer Res.* **48**, 7184–7188.
- Murata T., Goshima F., Daikoku T., Inagaki-Ohara K., Takakuwa H., Kato K. and Nishiyama Y. (2000) Mitochondrial distribution and function in herpes simplex virus-infected cells. *J. Gen. Virol.* **81**, 401–406.
- Nangaku M., Sato-Yoshitake R., Okada Y., Noda Y., Takemura R., Yamazaki H. and Hirokawa N. (1994) KIF1B, a novel microtubule plus end-directed monomeric motor protein for transport of mitochondria. *Cell* **79**, 1209–1220.
- Nicholls D. G. and Budd S. L. (2000) Mitochondria and neuronal survival. *Physiol. Rev.* **80**, 315–360.
- Nicholls D. G. and Scott I. D. (1980) The regulation of brain mitochondrial calcium-ion transport. The role of ATP in the discrimination between kinetic and membrane-potential-dependent calcium-ion efflux mechanisms. *Biochem. J.* **186**, 833–839.
- Nicholls D. G. and Ward M. W. (2000) Mitochondrial membrane potential and neuronal glutamate excitotoxicity: mortality and millivolts. *Trends Neurosci.* **23**, 166–174.
- Padua R. A., Baron K. T., Thyagarajan B., Campbell C. and Thayer S. A. (1998) Reduced Ca^{2+} uptake by mitochondria in pyruvate dehydrogenase-deficient human diploid fibroblasts. *Am. J. Physiol.* **43**, C615–C622.
- Petronilli V., Penzo D., Scorrano L., Bernardi P. and Di Lisa F. (2001) The mitochondrial permeability transition, release of cytochrome *c* and cell death. Correlation with the duration of pore openings *in situ*. *J. Biol. Chem.* **276**, 12030–12034.
- Pivovarov N. B., Hongpaisan J., Andrews S. B. and Friel D. D. (1999) Depolarization-induced mitochondrial Ca accumulation in sympathetic neurons: spatial and temporal characteristics. *J. Neurosci.* **19**, 6372–6384.
- Rappaport L., Oliviero P. and Samuel J. L. (1998) Cytoskeleton and mitochondrial morphology and function. *Mol. Cell. Biochem.* **184**, 101–105.
- Rizzuto R., Brini M., Murgia M. and Pozzan T. (1993) Microdomains with high Ca^{2+} close to IP_3 -sensitive channels that are sensed by neighboring mitochondria. *Science* **262**, 744–747.
- Rizzuto R., Brini M., Pizzo P., Murgia M. and Pozzan T. (1995) Chimeric green fluorescent protein as a tool for visualizing subcellular organelles in living cells. *Curr. Biol.* **5**, 635–642.
- Rizzuto R., Pinton P., Carrington W., Fay F. S., Fogarty K. E., Lifshitz L. M., Tuft R. A. and Pozzan T. (1998) Close contacts with the endoplasmic reticulum as determinants of mitochondrial Ca^{2+} responses. *Science* **280**, 1763–1766.
- Rizzuto R., Bernardi P. and Pozzan T. (2000) Mitochondria as all-round players of the calcium game. *J. Physiol. (Lond.)* **529**, 37–47.
- Sattler R., Xiong Z., Lu W. Y., Hafner M., MacDonald J. F. and Tymianski M. (1999) Specific coupling of NMDA receptor activation to nitric oxide neurotoxicity by PSD-95 protein. *Science* **284**, 1845–1848.
- Schatz G. and Dobberstein B. (1996) Common principles of protein translocation across membranes. *Science* **271**, 1519–1526.
- Schinder A. F., Olson E. C., Spitzer N. C. and Montal M. (1996) Mitochondrial dysfunction is a primary event in glutamate neurotoxicity. *J. Neurosci.* **16**, 6125–6133.
- Smirnova E., Shurland D. L., Ryazantsev S. N. and van der Bliek A. M. (1998) A human dynamin-related protein controls the distribution of mitochondria. *J. Cell Biol.* **143**, 351–358.
- Tang Y. G. and Zucker R. S. (1997) Mitochondrial involvement in post-tetanic potentiation of synaptic transmission. *Neuron* **18**, 483–491.
- Thayer S. A., Sturek M. and Miller R. J. (1988) Measurement of neuronal Ca^{2+} transients using simultaneous microfluorimetry and electrophysiology. *Pflugers Arch.* **412**, 216–223.
- Thayer S. A., Usachev Y. M. and Pottorf W. J. (2002) Modulating Ca^{2+} clearance from neurons. *Front. Biosci.* **7**, D1255–D1279.
- Usachev Y. M., DeMarco S. J., Campbell C., Strehler E. E. and Thayer S. A. (2002) Bradykinin and ATP accelerate Ca^{2+} efflux from rat sensory neurons via protein kinase C and the plasma membrane Ca^{2+} pump isoform 4. *Neuron* **33**, 113–122.
- Wang G. J. and Thayer S. A. (1996) Sequestration of glutamate-induced Ca^{2+} loads by mitochondria in cultured rat hippocampal neurons. *J. Neurophysiol.* **76**, 1611–1621.
- Wang G. J. and Thayer S. A. (2002) NMDA-induced calcium loads recycle across the mitochondrial inner membrane of hippocampal neurons in culture. *J. Neurophysiol.* **87**, 740–749.
- Werth J. L. and Thayer S. A. (1994) Mitochondria buffer physiological calcium loads in cultured rat dorsal root ganglion neurons. *J. Neurosci.* **14**, 348–356.
- Werth J. L., Usachev Y. M. and Thayer S. A. (1996) Modulation of calcium efflux from cultured rat dorsal root ganglion neurons. *J. Neurosci.* **16**, 1008–1015.
- White R. and Reynolds I. (1995) Mitochondria and $\text{Na}^+/\text{Ca}^{2+}$ exchange buffer glutamate-induced calcium loads in cultured cortical neurons. *J. Neurosci.* **15**, 1318–1328.
- Witners G. S. and Banker G. (1998) Characterizing and studying neuronal cultures, in *Culturing Nerve Cells. 2nd edition* (Banker G. and Goslin K. eds), pp. 113–151, MIT Press, Cambridge.
- Xia Z. G., Dudek H., Miranti C. K. and Greenberg M. E. (1996) Calcium influx via the nmda receptor induces immediate early gene transcription by a map kinase/erk-dependent mechanism. *J. Neurosci.* **16**, 5425–5436.
- Yaffe M. P. (1999) The machinery of mitochondrial inheritance and behavior. *Science* **283**, 1493–1497.